THE JOURNAL OF BIOLOGICAL CHEMISTRY VOL. 284, NO. 6, pp. 3537–3545, February 6, 2009
Printed in the U.S.A.

Oxidative Stress Alters Syndecan-1 Distribution in Lungs with Pulmonary Fibrosis*[S]

Received for publication, September 9, 2008, and in revised form, November 7, 2008 Published, JBC Papers in Press, December 9, 2008, DOI 10.1074/jbc.M807001200

Corrine R. Kliment[‡], Judson M. Englert[‡], Bernadette R. Gochuico[§], Guoying Yu[¶], Naftali Kaminski[¶], Ivan Rosas[‖], and Tim D. Oury[‡1]

From the [‡]Department of Cellular & Molecular Pathology and the [¶]Pulmonary Division, Department of Medicine, University of Pittsburgh School of Medicine, Pittsburgh, Pennsylvania 15213, the [§]National Human Genome Research Institute, National Institutes of Health, Bethesda, Maryland 20892, and the [‖]Pulmonary Division, Brigham and Women's Hospital, Boston, Massachusetts 02115

Idiopathic pulmonary fibrosis (IPF) is an interstitial lung disease characterized by severe, progressive fibrosis. Roles for inflammation and oxidative stress have recently been demonstrated, but despite advances in understanding the pathogenesis, there are still no effective therapies for IPF. This study investigates how extracellular superoxide dismutase (EC-SOD), a syndecan-binding antioxidant enzyme, inhibits inflammation and lung fibrosis. We hypothesize that EC-SOD protects the lung from oxidant damage by preventing syndecan fragmentation/shedding. Wild-type or EC-SOD-null mice were exposed to an intratracheal instillation of asbestos or bleomycin. Western blot was used to detect syndecans in the bronchoalveolar lavage fluid and lung. Human lung samples (normal and IPF) were also analyzed. Immunohistochemistry for syndecan-1 and EC-SOD was performed on human and mouse lungs. *In vitro*, alveolar epithelial cells were exposed to oxidative stress and EC-SOD. Cell supernatants were analyzed for shed syndecan-1 by Western blot. Syndecan-1 ectodomain was assessed in wound healing and neutrophil chemotaxis. Increases in human syndecan-1 are detected in lung homogenates and lavage fluid of IPF lungs. Syndecan-1 is also significantly elevated in the lavage fluid of EC-SOD-null mice after asbestos and bleomycin exposure. On IHC, syndecan-1 staining increases within fibrotic areas of human and mouse lungs. *In vitro*, EC-SOD inhibits oxidant-induced loss of syndecan-1 from A549 cells. Shed and exogenous syndecan-1 ectodomain induce neutrophil chemotaxis, inhibit alveolar epithelial wound healing, and promote fibrogenesis. Oxidative shedding of syndecan-1 is an underlying cause of neutrophil chemotaxis and aberrant wound healing that may contribute to pulmonary fibrosis.

Idiopathic pulmonary fibrosis (IPF)[2] is an interstitial lung disease characterized by severe and progressive fibrosis. IPF patients have a mean survival of 3–5 years (1, 2) and no effective therapies (3, 4), other than orthotopic lung transplantation, have proven to improve survival. The pathogenesis of IPF is poorly understood; however, inflammation and oxidant/antioxidant imbalances in the lung are thought to play important roles (5–7). A better understanding of the molecular mechanisms involved in oxidative injury and fibrosis could lead to the development of novel therapeutic targets.

Extracellular superoxide dismutase (EC-SOD) is an antioxidant enzyme bound to heparan sulfate in the lung extracellular matrix (8–10), which can inhibit inflammation (11, 12) and prevent subsequent development of fibrosis (13–16). Despite its beneficial role, the mechanisms through which EC-SOD protects the lung remain unknown.

The extracellular matrix (ECM) is essential for tissue homeostasis and changes in the ECM microenvironment can be detrimental to cell function during inflammation and wound healing. Heparan sulfate proteoglycans (HSPG) contain a membrane-bound core protein and extracellular carbohydrate side chains. Syndecans are the most abundant HSPG in humans; there are 4 isoforms with variable cell expression (17, 18). Both syndecan-1 and -4 are expressed in the lung, with epithelial cell and ubiquitous expression, respectively (19). Syndecans are essential for ECM homeostasis by binding cytokines and growth factors, acting as co-receptors and soluble effectors. They also have potential roles in inflammation (18, 20, 21), fibrosis (22, 23), and wound healing (24–26). Syndecans are shed under physiological and pathological conditions but the function of shed syndecans is poorly understood (22). Reactive oxygen species (ROS) are capable of fragmenting HSPG (27) and other ECM components. Notably, EC-SOD has been shown to prevent oxidative damage to many ECM components (23, 28, 29). Within the lung, EC-SOD binds to syndecan-1 on the cell surface via a heparin-binding domain (8, 30). Because of the known functions of syndecans and its close interaction with EC-SOD, syndecan-1 is a key target that

* This work was supported, in whole or in part, by the National Institutes of Health under a Ruth L. Kirschstein National Research Service Award (1F30ES016483-01, to C. R. K.), a Research Project Grant (R01HL063700-07, to T. D. O.), and by the Intramural Research Program of the NGRI and NHLBI. The costs of publication of this article were defrayed in part by the payment of page charges. This article must therefore be hereby marked "*advertisement*" in accordance with 18 U.S.C. Section 1734 solely to indicate this fact.

[S] The on-line version of this article (available at http://www.jbc.org) contains supplemental Figs. E1–E3.

[1] To whom correspondence should be addressed: Dept. of Pathology, University of Pittsburgh, 200 Lothrop St., Biomedical Sciences Tower W904, Pittsburgh, PA 15261. Tel.: 412-624-8888; Fax: 412-648-9172; E-mail: tdoury@pitt.edu.

[2] The abbreviations used are: IPF, idiopathic pulmonary fibrosis; EC-SOD, extracellular superoxide dismutase; ECM, extracellular matrix; GST, glutathione *S*-transferase; ROS, reactive oxygen species; HSPG, heparan sulfate proteoglycans; hS1ED, syndecan-1 ectodomain; siRNA, small interfering RNA; TGF, transforming growth factor.

may contribute to the anti-inflammatory and anti-fibrotic effects of EC-SOD in the lung and in the pulmonary fibrosis.

This study was conducted to determine the role of EC-SOD in protecting the ECM from oxidative stress and to investigate our hypothesis that EC-SOD protects the lung from inflammation and fibrosis by inhibiting oxidant-induced shedding of syndecan-1. Our findings suggest that a loss of EC-SOD in the lung leaves syndecan-1 vulnerable to oxidative stress and that oxidatively shed syndecan-1 ectodomain induces neutrophil chemotaxis, impairs epithelial wound healing, and promotes fibrogenesis. The discovery that oxidative stress alters the distribution of syndecan-1 in the lung microenvironment is a novel finding in the context of pulmonary fibrosis. These findings advance the understanding of the pathogenesis of idiopathic pulmonary fibrosis and provide a potential new therapeutic target for intervention in IPF.

MATERIALS AND METHODS

Animal Treatments—Animal protocols were approved by the University of Pittsburgh IACUC. Wild-type C57BL/6 and EC-SOD-null mice (EC-SOD KO) (13) were treated intratracheally with 0.1 mg of crocidolite asbestos or titanium dioxide (inert control particle), as previously described (15, 23). Select studies at the 1 day time point included co-treatment with asbestos and 50 units purified human EC-SOD (30, 31). 1, 14, and 28 days after treatment, bronchoalveolar lavage fluid (BALF) was recovered, and lungs were processed (32). Lungs were flash-frozen and homogenized for Western blot. Additional mice were treated intratracheally with 0.05 units of bleomycin and processed 7 days after treatment in the same manner as the asbestos experiments (14).

Human Samples—Human BALF and paraffin-embedded lung samples from IPF, and normal lungs were obtained at the Clinical Center, National Institutes of Health (NIH), in Bethesda, MD or at the University of Pittsburgh. IPF and control tissue samples for lung homogenates were obtained through the University of Pittsburgh Health Sciences Tissue Bank, as previously described (33). The use of these samples has been approved by the NHLBI and NHGRI of the National Institutes of Health, or the University of Pittsburgh IRBs. Lung homogenate samples were obtained from surgical remnants of biopsies or lungs explanted from patients with IPF who underwent pulmonary transplant. The homogenization process was the same as used for human lung samples described above. All patients fulfilled the diagnostic criteria for IPF outlined by the American Thoracic Society and European Respiratory Society (34). For immunohistochemistry, see the section below.

Western Blotting—BALF and lung homogenate proteins were separated by SDS-PAGE and transferred to polyvinylidene difluoride membranes (14, 23) and probed for proteins of interest. Membranes were probed with a rat anti-mouse antibody against syndecan-1 ectodomain (281.2, BD Biosciences) or mouse anti-human syndecan-1 (B-A38, Diaclone, Besancon, France), then a horseradish peroxidase (HRP)-conjugated donkey anti-rat and anti-mouse secondary antibodies (Jackson ImmunoResearch, West Grove, PA). ECL detection reagents were used for visualization (ECL-plus, GE Healthcare). Ponceau red membrane staining was used for BALF protein normalization and β-actin densitometry was used to normalize homogenates. Images were captured with a Gel Logic 2200 system for densitometry (mean normalized net intensities $\pm$S.E.).

Real Time PCR—RT-PCR was used to determine mRNA expression (ddCt relative quantitation) of EC-SOD from wild-type mice treated with TiO_2 or asbestos (14-day time point) and syndecan-1 from wild-type and EC-SOD KO mice treated with TiO_2 (day 14), using a 7300 Applied Biosystem PCR System and primer/probe sets (EC-SOD-Mm00448831_s1; syndecan-1-Mm00448918_m1 Sdc1, Applied Biosystems) as previously described (35). Data are reported as percent expression (relative to GAPDH expression) *versus* control, $n = 4$ samples per group, per gene.

Immunohistochemistry—Mouse lungs were inflation-fixed with 10% buffered formalin and paraffin-embedded. Paraffin-embedded IPF and control human lungs were also examined. 5-μm-thick sections of tissue were heated at 60 °C overnight, deparaffinized with xylene, rehydrated with an ethanol series, and fluorescently stained for syndecan-1 and EC-SOD. Human and mouse lung sections were stained with antibodies specific to syndecan-1 (1:500, B-A38, Abcam, Cambridge, MA; mouse: 281.2, BD Bioscience) and EC-SOD (1:500, generated as described below) and secondary antibodies labeled with Cy3 and Alexa 488 (1:5,000, Jackson Immunoresearch, Westgrove, PA). Control sections were stained with preimmune sera or non-immune IgG.

Generation of Anti-EC-SOD Antibodies—Mouse and human EC-SOD specific polyclonal antibodies were generated by immunizing rabbits with a keyhole limpet hemocyanin (KLH)-conjugated peptide containing either the first 19 amino acids in mouse EC-SOD and an additional cysteine residue at position 20 (SSFDLADRLDPVEKIDRLDC) or a peptide containing human EC-SOD amino acid residues 19–37 and an additional cysteine residue in position 20 (WTGEDSAEPNSDSAEWIRDC) by AnaSpec Corporation (San Jose, CA). Antibody specificity for EC-SOD was confirmed by the detection on a Western blot analysis of lung homogenate. Preimmune serum was also collected to obtain control IgG.

Cell Culture—Primary mouse alveolar epithelial cells were harvested and cultured from 6-week-old C57BL-6 mice, as previously described (36) and grown on collagen IV-coated 24-well plates for experiments in growth medium (Dulbecco's modified Eagle's medium with 10% fetal bovine serum, 50 international units/ml penicillin, 50 μg/ml streptomycin, Invitrogen). A549, human alveolar epithelial cells (ATCC), and LL47, human lung fibroblasts (ATCC), were separately grown on 24-well plates with growth medium for experiments (F12K medium with 10% fetal bovine serum; Invitrogen). A glutathione *S*-transferase (GST)-human syndecan-1 ectodomain fusion protein (hS1ED) was used in cell experiments at concentrations between 500 ng/ml and 1 μg/ml (provided by Dr. Alan Rapraeger and purified as previously described (37)). The present studies focus on the functions of the ectodomain protein itself, as there are no glycosaminoglycan chains present on the protein.

Fibroblast Proliferation and TGF-ß1 Release—LL47 fibroblasts were plated on 96-well plates (4,000 cells/well) and placed in serum-free F12K medium 24 h prior to treatment. Cells were treated with medium or 1 μg/ml hS1ED for 24 h at

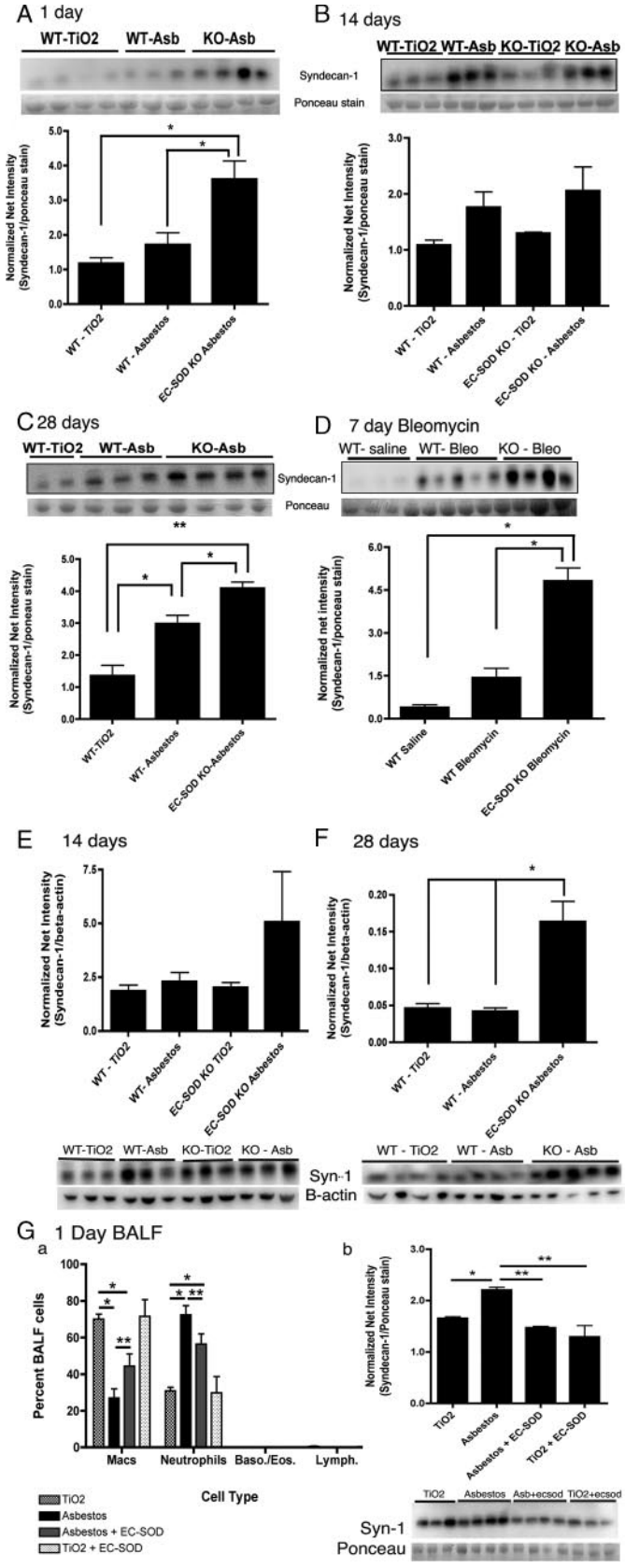

FIGURE 1. **Lack of EC-SOD leads to significant increases of syndecan-1 in bronchoalveolar lavage fluid (BALF) and lung tissue after asbestos or bleomycin exposure.** Syndecan-1 in the BALF and lung homogenates of wild type and EC-SOD KO mice was detected by Western blot analysis and presented as normalized net intensity (mean ±S.E.), $n = 5$ mice per group. Results for the BALF data are standardized to protein loading as determined by Ponceau red staining of the membrane. Results from lung homogenates are standardized to β-actin. Shed syndecan-1 in the BALF at: (*A*) 1-day post-asbestos exposure, *, $p < 0.05$; (*B*) 14-days post-asbestos exposure, *, $p < 0.05$; (*C*) 28-days post-asbestos exposure, *, $p < 0.05$, **, $p < 0.001$; and (*D*) 7-days post-bleomycin exposure, *, $p < 0.001$. *E*, syndecan-1 in lung homogenates at 14-days post-asbestos exposure and (*F*) 28 days post-asbestos exposure, *, $p < 0.05$. Co-treatment of EC-SOD KO mice with asbestos and purified EC-SOD results in *G–a* decreased neutrophils, *, $p < 0.001$; **, $p < 0.05$; and in *G-b* decreased levels of syndecan-1, *, $p < 0.05$; **, $p < 0.01$, in the BALF at day 1, $n = 4$.

37 °C/5% CO_2. Fibroblast proliferation was determined over 2 h using CellTiter 96 AQ Non-Radioactive Assay at 333 μg/ml MTS and 25 μM PMS (Promega, Madison, WI). Absorbance at 490 nm, which is proportional to the number of metabolically active cells, was recorded on a plate reader, and reported as mean ±S.E., $n = 8$. LL47s were also cultured to confluency on 12 well polystyrene plates, placed in serum-free medium for 24 h, and treated with 1 μg/ml hS1ED for 48 h. Supernatants were collected and assayed by ELISA for latent and active TGF-ß1 (R&D Systems, Minneapolis, MN). For α-smooth muscle actin (α-SMA) detection, fibroblast cell lysates were collected in ice-cold cell lysis buffer with protease inhibitors and separated on SDS page. After transfer to a membrane, mouse anti-α-SMA primary antibody (Sigma) was used for detection and normalized to β-actin as described.

Neutrophil Chemotaxis—A modified Boyden chamber (38), was used to evaluate human neutrophil (PMN) chemotaxis in response to shed syndecan-1 ectodomains in A549 cell supernatants, hS1ED (1 μg/ml), or heparan sulfate proteoglycan (HSPG, 6 μg/ml, Sigma). Samples were treated with reactive oxygen species (ROS) as previously described (23), purified human EC-SOD (30, 31) or CuZn-SOD (Alexis, San Diego, CA). ROS were generated in sterile HBSS using 1.25 μM copper sulfate (0.1 M NaH_2PO_4/50 μM $CuSO_4$; pH 7.4) and 1.5 mM hydrogen peroxide in a Fenton chemistry-like system (23, 28, 29, 39). Our previous studies (23) have shown that 0.068 nmol/min/ml superoxide are generated at the doses utilized in this study. Human PMN were isolated using a citrate and percoll isolation protocol (40) and 2×10^6 cells in HBSS were added to upper transwell inserts (5 μm pore size, Corning Inc., Corning, NY). Lower wells contained HBSS (Sigma) with the indicated treatments and incubated for 2 h. For select experiments, A549 cell monolayers were treated with medium, human syndecan-1 siRNA (sc-36587, Santa Cruz Biotechnology) or negative control siRNA (AM4611, Ambion) 24 h prior to ROS treatment to knockdown cell surface syndecan-1 expression. The optimal siRNA concentration was determined at 30 and 60 μM. A concentration of 30 μM was used for all additional experiments along with Lipofectamine 2000 (Invitrogen) and Opti-mem I (Invitrogen) reagents according to the manufacturer's protocol. Cells were then treated with ROS for 2 h at 37 °C/5% CO_2. Cell supernatants were collected and applied to the lower chamber of the chemotaxis assay. Neutrophils in the upper chambers were allowed to chemotax for 2 h at 37 °C/5% CO_2. Lower well cell counts were completed on a Beckmann Coulter Counter (Beckmann Coulter, Fullerton, CA). A migration index was calculated for each group (41; migrated cells to treatment/ran-

domly migrated cells (HBSS)). An index greater than 1 represents positive chemotaxis (±S.E.).

Shedding and Wound Assays—For shedding assays, A549 cells were exposed to ROS and EC-SOD for 30 min at 37 °C/5% CO_2. Cells were immunofluorescently stained for syndecan-1 (42), and supernatants were analyzed for shed syndecan-1 ectodomain by dot blot and by a syndecan-1 ELISA kit (anti-CD138, syn-1, Diaclone, France). Apoptosis, via caspase-3 activity, was assayed in 10 μg of A549 cell lysates using fluorogenic caspase-3 substrate IV, after ROS treatment and reported as mean relative fluorescent units, RFUs ±S.E. (Calbiochem, San Diego, CA). For wound assays, primary mouse alveolar epithelial cells or A549s were plated on collagen IV-coated plates and grown to confluency in growth media. Straight wounds were created with a p-200 pipette tips (43), washed, and treated with hS1ED (500 ng/ml or 1 μg/ml) immediately after wounding. Images were captured using a 4× objective with phase contrast at time 0 and 18, or 20 h. Human syndecan-1 siRNA (Santa Cruz Biotechnology) and negative control (scrambled) siRNA (Ambion) were used to knockdown syndecan-1 expression in A549 cells as described above. For siRNA experiments, wounds were created 24 h after siRNA treatment, and hS1ED (1 μg/ml) was added immediately after the wound was created and washed. Metamorph Software (Molecular Devices, Downingtown, PA) was used to measure wound areas. Results are presented as the percent wound healing. Percent healing was calculated as follows: (Wound Area (initial) − Wound Area-(final))/Wound area(initial) × 100.

Statistical Analysis—Mean densitometry and all other quantitative data (mean ±S.E.) were assessed for significance using the Student's t test or analysis of variance followed by Tukey's post-test using Graphpad Prism software (Graphpad, San Diego, CA). Significance was achieved by a p value < 0.05. Sample sizes (n) are indicated in the figure legends.

RESULTS

Syndecan-1 Ectodomain Shedding Increases after Asbestos-induced Lung Injury in Mice—To investigate syndecan-1 ectodomain shedding in models of pulmonary fibrosis, we measured shed syndecan-1 protein levels in the bronchoalveolar lavage fluid (BALF) of wild-type and EC-SOD-null mice (EC-SOD KO) in both asbestos and bleomycin-induced models of pulmonary fibrosis. EC-SOD KO mice are more susceptible to oxidative damage and lung fibrosis (13–15, 34). After asbestos injury, shed syndecan-1 levels increase in the BALF of wild-type mice at 1, 14, and 28 days post-asbestos exposure (Fig. 1, *A–C*, $n = 5$). Notably, shedding of syndecan-1 from the ECM after asbestos injury was significantly ($p < 0.05$) further increased in mice lacking EC-SOD at days 1 and 28 (EC-SOD KO mice, Fig. 1, *A* and *C*). Syndecan-1 was also found to significantly ($p < 0.05$) increase in lung homogenates at 28 days post-asbestos exposure, with the trend beginning at 14-days post-exposure (Fig. 1, *E* and *F*, $n = 4–5$). Similar results were observed in a bleomycin model of pulmonary fibrosis. Shed syndecan-1 levels significantly ($p < 0.001$) increase in the BALF of EC-SOD-KO mice when compared with wild-type mice at 7 days after bleomycin treatment (Fig. 1*D*, $n = 5$). Furthermore, in EC-SOD KO mice at the 24-h time point,

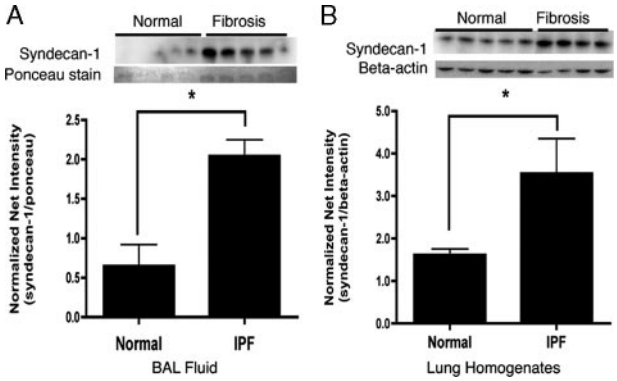

FIGURE 2. **Syndecan-1 increases in the BALF and lung homogenates of IPF lungs compared with normal.** Syndecan-1 was detected by Western blot analysis and presented as normalized net intensity (standardized to protein loading as determined by Ponceau red staining of the membrane for BALF samples and standardized to β-actin for lung homogenate samples (mean ±S.E.). Increased syndecan-1 in (*A*) BALF samples; *, $p < 0.01$, $n = 5$ and (*B*) lung homogenate samples; *, $p < 0.05$, $n = 4–5$.

co-treatment with asbestos and 50 units EC-SOD intratracheally results in a significant decrease in neutrophils ($p < 0.05$; Fig. 1, *G–a*) and a decrease in shed syndecan-1 in the BALF ($p < 0.01$; Fig. 1, *G–b*).

Syndecan-1 Ectodomain Levels Increase in IPF—To determine if syndecan-1 shedding also occurs in subjects affected with IPF, we measured syndecan-1, by Western blot analysis, in BALF and lung homogenates obtained from patients who met ATS/ERS criteria for sporadic IPF (34). Syndecan-1 levels were significantly increased in the BALF ($p < 0.01$) and lung homogenates ($p < 0.05$) of IPF patients when compared with control subjects (Fig. 2*A*).

Syndecan-1 Is Increased in Fibrotic Lung Regions and Co-localizes with EC-SOD—To further evaluate syndecan-1 expression in response to pulmonary fibrosis, immunofluorescent staining for syndecan-1 and EC-SOD was performed on human and mouse lungs with and without fibrosis. Fig. 3*A* depicts lung sections of normal human lung and sporadic IPF. Normal human lung in Fig. 3, *A–a* shows ubiquitous staining for EC-SOD (*green*) with sparse staining for syndecan-1 (*red*), and co-localization of the two proteins (*yellow* with *arrows*). Similarly, in Fig. 3, *A–c*, an area of tissue with normal architecture from an IPF lung shows ubiquitous EC-SOD and sparse syndecan-1 staining. In contrast, Fig. 3*A*, *b* and *d*, depicts areas of fibrosis in IPF sections that stain strongly for syndecan-1 on the abluminal surface of alveolar epithelial cells, terminal bronchiolar epithelial cells, and within areas of fibrosis (*double asterisks*). EC-SOD staining decreases in fibrotic regions (Fig. 3, *A–b*, *single asterisk*) and co-localizes with syndecan-1 in the lung epithelium (Fig. 3, *A–d*, *arrows*). Areas of fibrosis were identified using H&E staining of serial lung sections by a board-certified pathologist.[3] Overall, in areas of fibrosis in IPF lung, there is an increase in syndecan-1 staining with a decrease in interstitial EC-SOD.

In the asbestos mouse model, the asbestos-induced injury leads to peribronchial and alveolar fibrosis similar to that seen in IPF. To confirm the human IHC staining results, mouse lung

[3] T. D. Oury, data not shown.

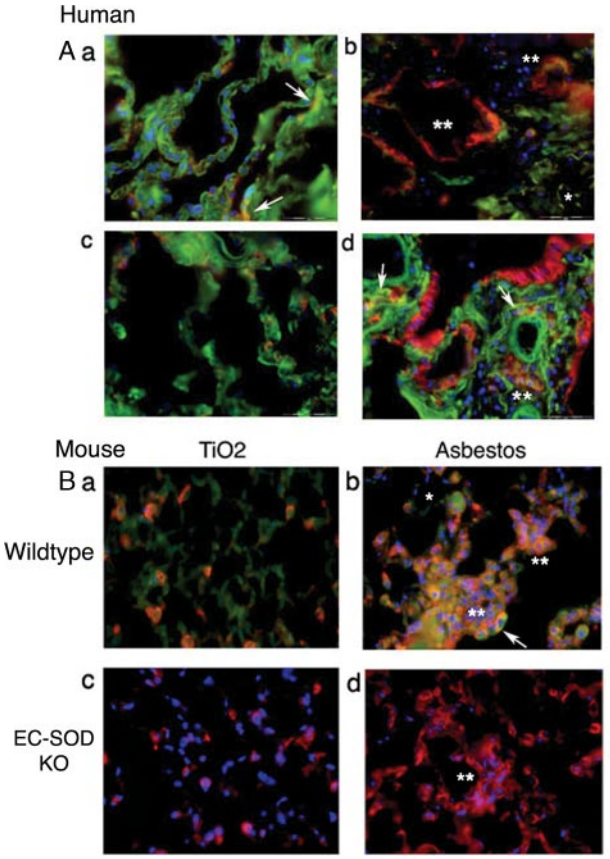

FIGURE 3. **Localization of EC-SOD and syndecan-1 in human and mouse lung sections.** *Green*, EC-SOD; *red*, syndecan-1; *blue*, nuclear stain; *yellow*, co-localization. *A*, human lung: there is diffuse expression of EC-SOD in the normal lung parenchyma (*a*) and focal areas of syndecan-1 expression co-localize with EC-SOD (*yellow*; *arrows*). Areas of normal lung architecture in IPF lungs (*c*) show similar labeling for both EC-SOD and syndecan-1. In contrast, areas with fibrosis (*b* and *d*) show increased staining for syndecan-1 (*red staining*, *asterisks*), decreased EC-SOD (green staining, single asterisk), and only a minor portion of this syndecan-1 still co-localizes with EC-SOD (*yellow staining*, *arrows*). *B*, lung tissue of wild-type and EC-SOD KO mice treated with asbestos or TiO_2 at 28-days post-exposure. *a*, normal lung architecture of TiO_2 treated wild-types show diffuse EC-SOD staining (*green*) and focal syndecan-1 expression that co-localizes with EC-SOD (*orange/yellow*) similar to that seen in human lungs. *b*, fibrotic areas of asbestos treated wild-type mice show increased diffuse syndecan-1 staining (*double asterisks*) that co-localizes with EC-SOD (*yellow*, *arrows*). EC-SOD KO mouse lungs were stained for syndecan-1 depicting (*c*) normal lung architecture after TiO_2 treatment (H&E image found in supplemental Fig. E2) and (*d*) fibrosis after asbestos treatment. There are significant increases in diffuse syndecan-1 staining in areas of fibrosis (*double asterisks*). No staining was seen with non-immune sera or IgG control staining, see supplemental Fig. E1.

sections were stained for EC-SOD and syndecan-1 after TiO_2 or asbestos exposure (28-day time point). Fig. 3, *B–a* shows diffuse EC-SOD staining (*green*) and sparse syndecan-1 (*red*) of normal lung in wild-type mice after TiO_2 exposure. In contrast, areas of fibrosis in Fig. 3, *B–b* show a diffuse increase in syndecan-1 (*double asterisks*), a decrease in interstitial EC-SOD (*single asterisk*), and co-localization of the two proteins in wild-type mice (*yellow* with *arrows*). Likewise, in EC-SOD KO mice, syndecan-1 expression significantly increases in areas of fibrosis after asbestos treatment (Fig. 3, *B–d*, *double asterisks*) compared with TiO2-treated mice (Fig. 3, *B–c*).

Previous studies demonstrate that EC-SOD decreases in the lung interstitium after fibrosis-inducing injury while increasing in the alveolar lining fluid, as determined by Western blot analysis of lung homogenates and BALF, respectively (15, 32). Real time PCR was used to confirm our IHC staining for EC-SOD in mouse lung. EC-SOD gene expression decreases significantly in wild-type mouse lungs after asbestos treatment at 14-days-post-exposure; percent EC-SOD gene expression from TiO_2-treated lungs: 100% ± 4.96 *versus* 76.32% ± 3.40 for asbestos-treated lungs ($p < 0.05$, $n = 4$). Syndecan-1 gene expression in the lung was not significantly different between TiO_2, control-treated wild-type mice (100% ± 4.51) and EC-SOD KO mice (99.46% ± 4.51) $p = 0.95$, $n = 4$. See online supplemental Fig. E3 for a graphical representation. This led us to hypothesize that the absence of EC-SOD may leave syndecan-1 vulnerable to oxidative stress and lead to shedding of membrane-bound syndecan-1.

EC-SOD Protects against Oxidative Shedding of Syndecan-1—To determine if oxidative stress leads to shedding of syndecan-1 *in vitro*, A549 cells (human alveolar epithelial cell line) were exposed to ROS in the presence or absence of human EC-SOD. A549 cells are sensitive to oxidative shedding of syndecan-1, as evidenced by a significant ($p < 0.05$) increase in levels of shed syndecan-1 in cell supernatants after treatment with ROS (Fig. 4*A*). ROS treatment does not induce apoptosis in the cells, as depicted by no changes in caspase-3 activity in cell lysates after ROS treatment (caspase-3 activity, RFUs: medium 657.1 ± 73.1 *versus* ROS 405.3 ± 75.1; $p = 0.074$, $n = 3$). Furthermore, treatment with EC-SOD can significantly ($p < 0.01$) protect these cells from ROS-induced syndecan-1 shedding. Consistent with these findings, we observed loss of cell surface syndecan-1 staining after ROS exposure suggesting that shedding was inhibited by treatment with EC-SOD (Fig. 4*B*). The concentrations of syndecan-1 in A549 cell supernatants after medium *versus* ROS treatment were determined by ELISA to be 9.2 ng/ml ± 2.3 and 42.3 ng/ml ± 1.9 ($p < 0.0001$), respectively.

Syndecan-1 Ectodomain and Heparan Sulfate Proteoglycan Promote Chemotaxis—Inflammatory cell influx is a feature in the pathogenesis of pulmonary fibrosis (6, 14, 15, 44). We have previously shown that heparan sulfate proteoglycans (HSPG), treated with ROS promote neutrophil chemotaxis, which is inhibited by the presence of EC-SOD (23). Because syndecan-1 is important in IPF and in mouse models of lung injury, we hypothesized that oxidatively shed syndecan-1 ectodomain and HSPG would promote neutrophil chemotaxis to the lung. The chemotactic properties of shed syndecan, HSPG, and hS1ED were evaluated *in vitro* with a modified Boyden-chamber system. As shown in Fig. 4*A*, syndecan-1 can be oxidatively shed from A549 cells. Supernatants containing shed syndecan-1 are chemotactic to neutrophils (Fig. 4*C*; migration index of ROS alone 1.70 ± 0.22 *versus* HBSS control 1.00 ± 0.10, $p < 0.001$, $n = 6$). Knockdown of syndecan-1 cell surface expression partially inhibits ROS-induced neutrophil chemotaxis (Fig. 4*C*; migration index of Syn1 siRNA with ROS 1.12 ± 0.07, $p < 0.001$ *versus* ROS alone 1.70 ± 0.22). Fig. 4*D* shows that HSPG does not cause chemotaxis alone. However, chemotaxis was induced by exposure of HSPG to ROS and was inhibited by the addition of EC-SOD at amounts of 5, 50, and 100 units per well (Fig. 4*D*). EC-SOD provides better protection for HSPG than CuZnSOD, which lacks the heparin-binding domain of EC-SOD. Chemotaxis induced by HSPG with ROS and 5 units or 100 units

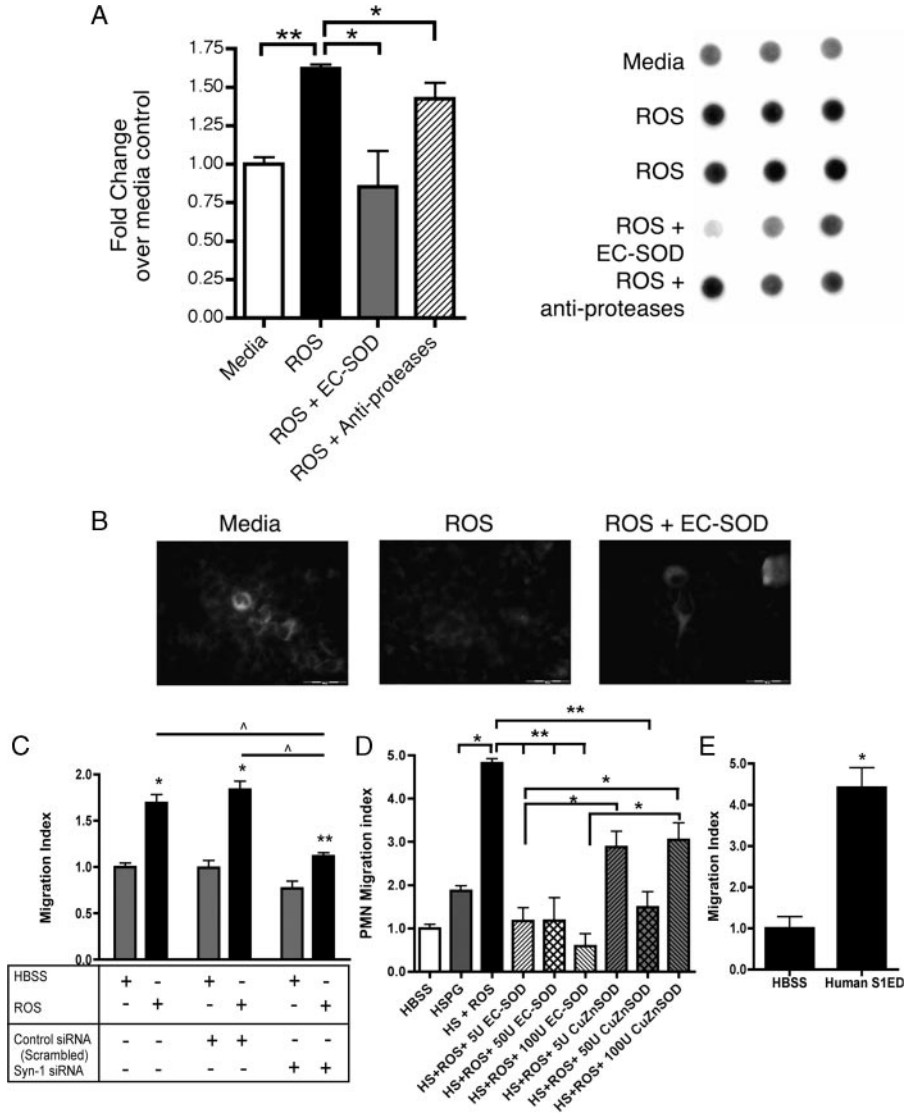

FIGURE 4. **EC-SOD protects against oxidative shedding of syndecan-1.** A549 cells were treated with ROS in the presence or absence of EC-SOD or CuZnSOD. *A*, dot blots of the culture medium were probed for human syndecan-1. Results are presented as fold increase in dot intensity over medium-treated controls (mean ±S.E.); *, $p < 0.05$; **, $p < 0.01$. *B*, representative fluorescent staining of syndecan-1 on A549 cells after treatment with ROS in the absence and presence of EC-SOD. *C*, supernatants from A549s treated with medium, control siRNA, or syn-1 siRNA 24 h prior to treatment with HBSS or ROS were used in the chemotaxis assay. Oxidatively shed syndecan-1, in the supernatants, is chemotactic to neutrophils (*PMN*). Knockdown of syndecan-1 expression inhibits chemotaxis after ROS treatment. *, $p < 0.001$ and **, $p < 0.01$ *versus* HBSS; ^, $p < 0.001$. *D*, oxidatively fragmented heparan sulfate proteoglycan (*HSPG*) and (*E*) unmodified hS1ED promote chemotaxis of PMNs ($n = 6$, *, $p < 0.005$). Data are reported as a PMN migration index (±S.E.). Treatments were completed in triplicate. Data are representative of three separate experiments.

CuZnSOD is not significantly different from HSPG with ROS alone. hS1ED (1 μg/ml) alone caused chemotaxis of human neutrophils (Fig. 4*E*, HBSS 1.0 ± 0.49 *versus* hS1ED 4.42 ± 0.83, $p < 0.005$). ROS, H_2O_2, human EC-SOD and CuZnSOD alone do not induce chemotaxis (not shown). Therefore, syndecan-1 ectodomain that is oxidatively shed and modified during lung injury is highly chemotactic to neutrophils.

Shed Syndecan-1 Ectodomain and Lack of Cell Surface Syndecan-1 Inhibit Wound Healing—Aberrant wound healing and a lack of re-epithelialization are key characteristics thought to be involved in IPF pathogenesis (45). To determine the effect of shed syndecan-1 on epithelial wound healing, an *in vitro* scratch assay was performed using cultured primary mouse alveolar epithelial cells and A549 cells.

In wounded primary alveolar epithelial cells, hS1ED, added at the time of the wound, significantly inhibited healing of monolayers after 20 h (Fig. 5*A*, percent healing ±S.E.): medium alone: 65.0% ± 3.7 healing *versus* 1 μg/ml hS1ED: 51.6% ±1.7, *, $p < 0.05$. Supernatants from A549 cells exposed to ROS inhibited re-epithelialization of A549 monolayers after wounding and led to a large decrease in cell adhesion after 20 h (data not shown). hS1ED added at the time of the wound also inhibited healing of A549 monolayers (control 92.4% ± 1.2 *versus* hS1ED (500 ng/ml) 73.5%±3.5, $p < 0.01$ Fig. 5, *B* and *C*). Both primary cells and A549s displayed a rounded, less adhered morphology after treatment with soluble syndecan-1 (data not illustrated). Knockdown of syndecan-1 expression in A549 cells was achieved with siRNA to human syndecan-1 (80% knockdown 24 h after siRNA treatment, Fig. 5*D*). The loss of syndecan-1 expression, 24-h-post-transfection, resulted in a significant decrease in alveolar epithelium wound healing (negative control siRNA 80.1% ± 6.6 *versus* syndecan-1 siRNA 49.3% ± 5.7, $p < 0.001$, Fig. 5, *B* and *C*). The addition of syndecan-1 ectodomain, hS1ED (1 μg/ml, immediately after wounding) to siRNA-treated cells did not significantly augment the impaired wound healing response.

Syndecan-1 Ectodomain Increases Fibroblast Proliferation and TGF-ß1 Release—To determine the effect of hS1ED on fibroblasts, LL47 cells (lung fibroblast cell line) were treated with 1 μg/ml hS1ED for 24 or 48 h and metabolically active cells were detected as described. hS1ED significantly increases the proliferation of lung fibroblasts after 24 h (Fig. 6*A*, $p < 0.01$, corrected absorbance: medium 0.50 ± 0.02 *versus* hS1ED 0.61 ± 0.04). Furthermore, hS1ED induces increased TGF-ß1 release by fibroblasts treated for 48 h (Fig. 6*B*, TGF-ß1(ng/ml): medium 0.34 ± 0.08 *versus* hS1ED 0.80 ± 0.05). There was no detectable increase in active TGF-ß1 (data not shown). Additional studies indicate that hS1ED does not lead to myofibroblast differentiation of fibroblasts, as determined by α-smooth muscle actin in cell lysates after treatment for 48 h (data not shown).

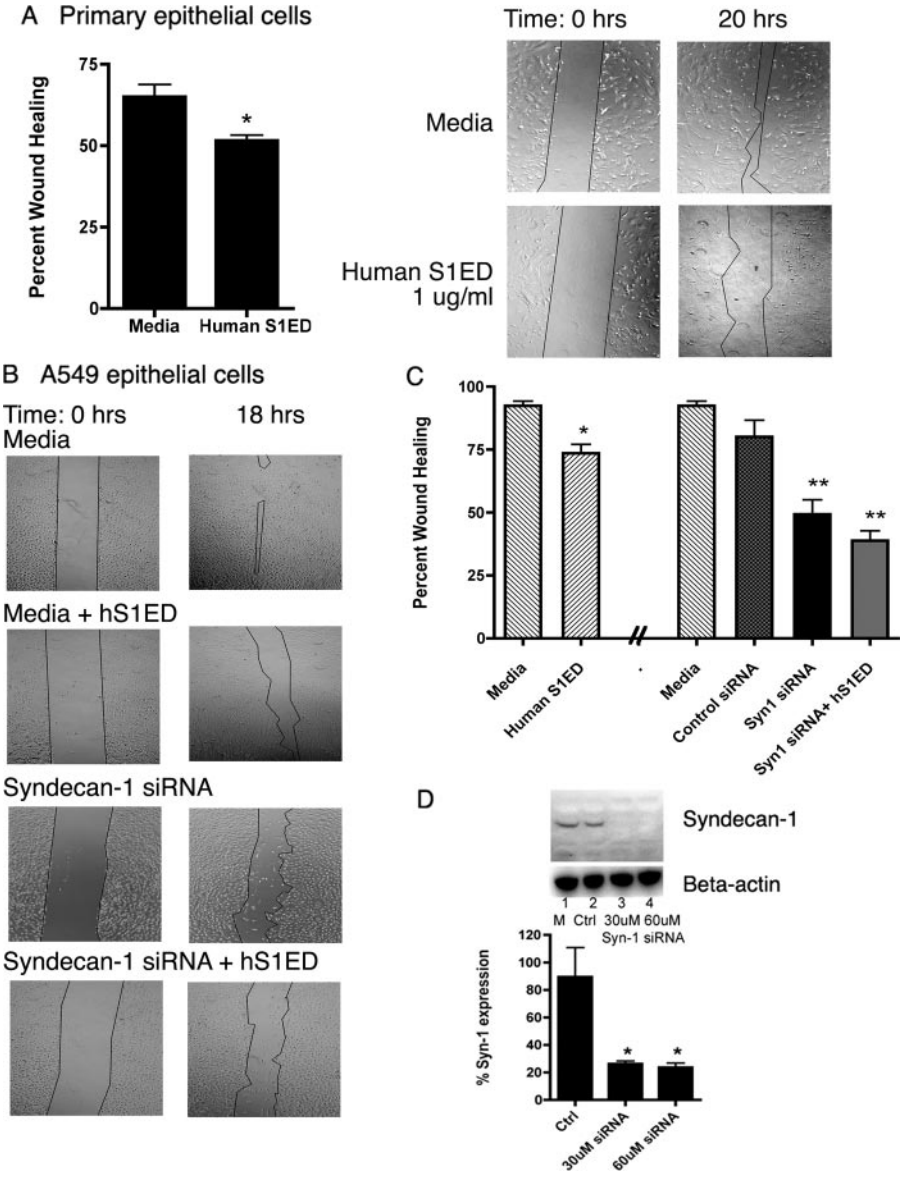

FIGURE 5. **hS1ED inhibits wound healing, while cell surface syndecan-1 promotes alveolar re-epithelialization.** Data are reported as percent wound healing (±S.E.), $n = 6$ per group. *A*, phase images of mouse primary alveolar epithelial cell monolayer wounds exposed to hS1ED, which inhibits primary cell wound healing over 20 h. *, $p < 0.05$. *B*, phase images of A549 monolayer wounds exposed to hS1ED, syndecan-1 siRNA or negative control siRNA (graphically represented as percent wound healing in *C*). hS1ED inhibits A549 epithelial wound healing over 18 h. Knockdown of syndecan-1 with 30 μM siRNA (siRNA treatment was given 24 h prior to the wound) results in impaired wound healing and changes to cell morphology from a flat, squamous shape to a rounded cell. *, $p < 0.05$; **, $p < 0.001$. There was no difference between baseline wound healing with medium and control siRNA. *D*, successful knockdown of human syndecan-1 in A549 cells by 30 μM and 60 μM syndecan-1 siRNA (24 h after siRNA treatment). *, $p < 0.05$.

DISCUSSION

Previous studies have demonstrated that EC-SOD inhibits inflammation and fibrosis in several models of pulmonary injury. In addition, interstitial EC-SOD is lost in response to many injuries that lead to pulmonary fibrosis (15, 32). This loss of interstitial EC-SOD may promote both inflammation and fibrosis after lung injury. The mechanisms through which EC-SOD inhibits inflammation and fibrosis are poorly understood. Recent reports suggest that a mechanism by which EC-SOD regulates inflammation is by inhibiting oxidative fragmentation of glycosaminoglycans such as hyaluronan and heparan sulfates (23, 29).

Syndecans are heparan sulfate proteoglycans that contribute to neutrophil chemotaxis, regulation of the ECM, cytokine and growth factor function, and cell adhesion (20, 25, 26, 46). Overall, the functions of syndecans are not completely understood and notably, the biological roles of their ectodomains change when shed into the tissue extracellular matrix (46). Because of the ability of EC-SOD to directly bind to heparan sulfate proteoglycans and inhibit oxidative fragmentation of these important matrix components, we hypothesized that protection of syndecans against oxidative modification is a mechanism through which EC-SOD inhibits inflammation and fibrosis in response to lung injury.

The present study demonstrates that shedding of syndecan-1 ectodomain may play a role in the development and progression of pulmonary fibrosis. More importantly, our results suggest a novel mechanism through which EC-SOD protects the lung against oxidative damage by inhibiting syndecan-1 ectodomain shedding. The current data indicate that syndecan-1 contributes to neutrophil chemotaxis, modulates re-epithelialization, and promotes fibrosis after lung injury.

The current studies show that there is increased syndecan-1 shedding into the BALF of mice following asbestos and bleomycin injury (Fig. 1). We have now shown that the shedding of syndecan-1 is significantly further increased in the BALF of EC-SOD KO mice in response to both asbestos injury and bleomycin injury. These findings are further supported by increases in shed syndecan-1 in the BALF of IPF patients (Fig. 2). Oxidative stress contributes to mouse models of fibrosis, IPF, and other pulmonary diseases (5, 47–49). We have demonstrated that EC-SOD inhibits syndecan-1 shedding and reduces BALF neutrophil influx *in vivo* (Fig. 1) and also inhibits syndecan-1 shedding *in vitro* (Fig. 4), suggesting that oxidative stress contributes to syndecan-1 shedding in fibrotic lungs and that EC-SOD can inhibit this shedding.

Inflammation and impaired epithelial wound healing are key pathological processes involved in both the animal models of pulmonary fibrosis and in IPF. The studies presented here sug-

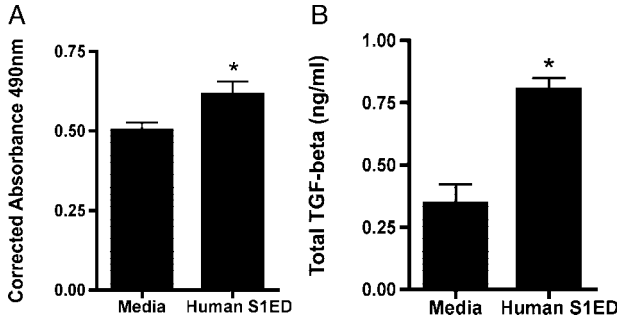

FIGURE 6. **Syndecan-1 ectodomain induces lung fibroblast proliferation and induces release of TGF-ß1.** *A*, LL47 fibroblasts were treated with medium or hS1ED for 24 h, and proliferation was determined. Corrected absorbance at 490 nm is proportional to the number of metabolically active cells. *, $p < 0.01$. *B*, fibroblasts were treated with medium or hS1ED for 48 h. Supernatants were subsequently assayed for total TGF-ß1 (ng/ml); *, $p < 0.01$. No differences in active TGF-ß1 levels were detected.

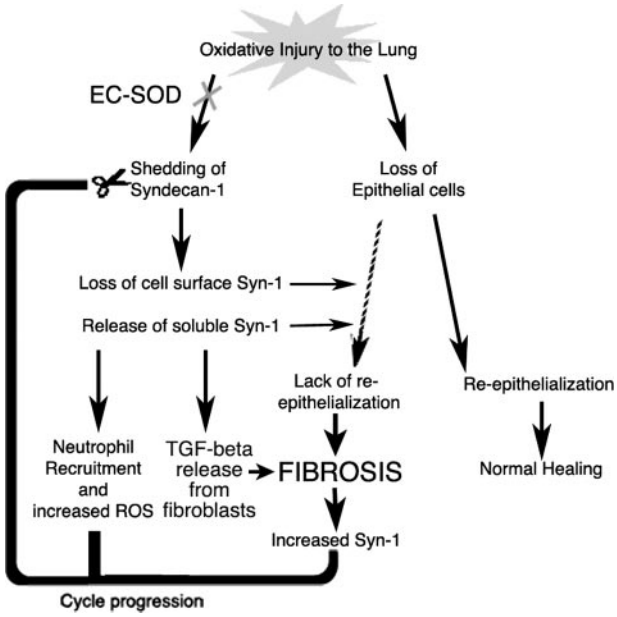

FIGURE 7. **Summary of oxidative stress in the lung.** Oxidative injury to the lung can lead to loss of epithelial cells and shedding of syndecan-1. This shedding may create a damaging cycle of cell chemotaxis, abnormal re-epithelialization, and increased TGF-β bioavailability that contribute to fibrosis development in the lung.

gest a novel mechanism by which oxidants induce shedding of syndecan-1 and that hS1ED can directly promote neutrophil chemotaxis in the absence of cytokines or chemokines. The neutrophil chemotaxis data show that oxidatively shed syndecan-1 from A549 cells induce chemotaxis, which was partially inhibited by knockdown of A549 syndecan-1 expression (Fig. 4*C*), suggesting that while other factors are contributing to neutrophil chemotaxis, the shed syndecan-1 ectodomain is a potent chemo-attractant. We confirmed the chemotactic response with hS1ED and heparan sulfate proteoglycan. hS1ED was directly chemotactic, (Fig. 4*E*) while HSPG was chemotactic after exposure to reactive oxygen species (Fig. 4*D*). Oxidative damage and removal of the carbohydrate side chains from HSPG can expose the syndecan core protein. The core syndecan protein is then able to induce chemotaxis. The mechanism in which shed syndecan-1 induces chemotaxis is not known, but toll-like receptor-4 may be involved as this receptor was previously shown to be involved in heparan sulfate-mediated neutrophil chemotaxis (23). Along with being involved in recognition of host invasion by Gram-negative bacteria, TLR-4 may recognize soluble syndecan-1 as a signal of tissue injury. This is the first report of direct-induction of chemotaxis by the syndecan-1 ectodomain in the context of fibrotic lung injury.

Other fibrosis studies have reported the involvement of specific inflammatory chemokines that localize to syndecans in the ECM to create chemotactic gradients (22). hS1ED and oxidatively fragmented HSPG may also independently create gradients that attract and activate neutrophils. A recent clinical study shows prognostic benefit to evaluating neutrophil burden in BAL fluid in IPF (50). Detecting increases in syndecan-1 in the BAL fluid in patients with pulmonary fibrosis may provide additional clinically relevant information on inflammatory and fibrotic mediators that are involved in IPF pathogenesis.

Wound healing studies suggest that in addition to pro-inflammatory properties, shed sydecan-1 impairs alveolar epithelial wound healing. These studies indicate that cell surface-bound syndecan-1 is important for re-epithelialization after injury, as siRNA inhibition of syndecan-1 expression significantly impaired healing (Fig. 5). In addition, hS1ED was found to inhibit wound healing at physiological syndecan-1 concentrations (Fig. 5). Decreased expression of cell-surface syndecan-1 resulted in a decrease in the ability of alveolar epithelial cells to heal a wounded area. The literature suggests that syndecan-1 interacts with various integrins to mediate integrin activation and enhance cell adhesion (37). In the present study, soluble syndecan-1 may be inhibiting re-epitheliation by competitively binding to integrin subunits.

Based on the data described, we hypothesize that syndecan-1 also modulates fibroblast proliferation and function. Syndecan-1 plays a role in cellular responsiveness to fibroblast growth factor, FGF (46) and cell adhesion and extension through integrins (37). hS1ED significantly increased the proliferation of human lung fibroblasts and increased their release of latent TGF-ß1 (Fig. 6). These data suggest that syndecan-1 ectodomain may also contribute to the development of pulmonary fibrosis by activating fibroblast growth and increasing the release of key pro-fibrotic mediators such as TGF-ß1.

Taken together, the findings of this study suggest that a loss of EC-SOD in the lung leaves syndecan-1 vulnerable to oxidative stress and that the oxidant-induced loss of cell surface syndecan-1 impairs re-epithelialization, induces neutrophil chemotaxis, and promotes a fibrotic microenvironment in the lung. Tissue homogenate, immunofluorescent staining, and real time PCR data indicate the presence of syndecan-1 cell surface expression in areas of fibrosis while EC-SOD decreases in the lung after injury. The loss of interstitial EC-SOD in response to asbestos and bleomycin injury may increase the vulnerability of matrix proteins and proteoglycans, including syndecan-1, to oxidative modification. The combination of these changes that occur in lung interstitial syndecan-1 and EC-SOD distribution may favor fibrogenesis by creating a cycle of sustained inflammatory cell recruitment, abnormal epithelial wound healing, and increased TGF-ß1 bioavailability (Fig. 7).

This study provides new insights into the role of EC-SOD in protecting the lung against oxidative damage and potential mechanisms by which shed syndecan-1 ectodomain can promote the development of pulmonary fibrosis. Taken together, these findings provide a general mechanism through which oxidative processes induce lung injury and provide incite for future investigations into the role of syndecan-1 in other oxidant-induced lung pathologies and diseases.

In conclusion, these studies show that shed syndecan-1 contributes to the pathogenesis of pulmonary fibrosis by inducing neutrophil chemotaxis, impairing re-epithelialization following alveolar injury, and promoting fibrogenesis. This study also highlights the importance of EC-SOD in preventing oxidant-induced shedding of syndecan-1 in the lung and illustrates that the loss of EC-SOD in response to pulmonary fibrosis leaves the ECM vulnerable to oxidative stress. These results provide insight into potential therapeutic avenues targeting oxidative changes occurring in the extracellular matrix of the lung in IPF.

Acknowledgments—We thank Dr. Alan Rapraeger, University of Wisconsin-Madison, for generously providing the GST syndecan-1 fusion protein (hS1ED) for this study. Technical support provided by Jacob Tobolewski and Beth Ganis is gratefully acknowledged.

REFERENCES

1. Dempsey, O. J. (2006) *Respir. Med.* **100,** 1871–1885
2. Flaherty, K. R., Travis, W. D., Colby, T. V., Toews, G. B., Kazerooni, E. A., Gross, B. H., Jain, A., Strawderman, R. L., Flint, A., Lynch, J. P., and Martinez, F. J. (2001) *Am. J. Respir. Crit. Care Med.* **164,** 1722–1727
3. Gross, T. J., and Hunninghake, G. W. (2001) *N. Engl. J. Med.* **345,** 517–525
4. Walter, N., Collard, H. R., and King, T. E., Jr. (2006) *Proc. Am. Thorac. Soc.* **3,** 330–338
5. Kinnula, V. L., Fattman, C. L., Tan, R. J., and Oury, T. D. (2005) *Am. J. Respir. Crit. Care Med.* **172,** 417–422
6. Obayashi, Y., Yamadori, I., Fujita, J., Yoshinouchi, T., Ueda, N., and Takahara, J. (1997) *Chest* **112,** 1338–1343
7. Ozaki, T., Hayashi, H., Tani, K., Ogushi, F., Yasuoka, S., and Ogura, T. (1992) *Am. Rev. Respir. Dis.* **145,** 85–91
8. Karlsson, K., Lindahl, U., and Marklund, S. L. (1988) *Biochem. J.* **256,** 29–33
9. Fattman, C. L., Schaefer, L. M., and Oury, T. D. (2003) *Free Radic Biol. Med.* **35,** 236–256
10. Oury, T. D., Day, B. J., and Crapo, J. D. (1996) *Lab. Investig.* **75,** 617–636
11. Bowler, R. P., Nicks, M., Tran, K., Tanner, G., Chang, L. Y., Young, S. K., and Worthen, G. S. (2004) *Am. J. Respir. Cell Mol. Biol.* **31,** 432–439
12. Folz, R. J., Abushamaa, A. M., and Suliman, H. B. (1999) *J. Clin. Investig.* **103,** 1055–1066
13. Carlsson, L. M., Jonsson, J., Edlund, T., and Marklund, S. L. (1995) *Proc. Natl. Acad. Sci. U. S. A* **92,** 6264–6268
14. Fattman, C. L., Chang, L. Y., Termin, T. A., Petersen, L., Enghild, J. J., and Oury, T. D. (2003) *Free Radic Biol. Med.* **35,** 763–771
15. Fattman, C. L., Tan, R. J., Tobolewski, J. M., and Oury, T. D. (2006) *Free Radic Biol. Med.* **40,** 601–607
16. Tan, R. J., Lee, J. S., Manni, M. L., Fattman, C. L., Tobolewski, J. M., Zheng, M., Kolls, J. K., Martin, T. R., and Oury, T. D. (2006) *Am. J. Respir. Cell Mol. Biol.* **34,** 226–232
17. Bernfield, M., Gotte, M., Park, P. W., Reizes, O., Fitzgerald, M. L., Lincecum, J., and Zako, M. (1999) *Annu. Rev. Biochem.* **68,** 729–777
18. Venkatesan, N., Roughley, P. J., and Ludwig, M. S. (2002) *Am. J. Physiol. Lung Cell Mol. Physiol.* **283,** L806–L814
19. Bernfield, M., Kokenyesi, R., Kato, M., Hinkes, M. T., Spring, J., Gallo, R. L., and Lose, E. J. (1992) *Annu. Rev. Cell Biol.* **8,** 365–393
20. Parish, C. R. (2005) *Nat. Immunol.* **6,** 861–862
21. Wang, L., Fuster, M., Sriramarao, P., and Esko, J. D. (2005) *Nat. Immunol.* **6,** 902–910
22. Li, Q., Park, P. W., Wilson, C. L., and Parks, W. C. (2002) *Cell* **111,** 635–646
23. Kliment, C. R., Tobolewski, J. M., Manni, M. L., Tan, R. J., Enghild, J., and Oury, T. D. (2008) *Antioxid. Redox Signal.* **10,** 261–268
24. Echtermeyer, F., Streit, M., Wilcox-Adelman, S., Saoncella, S., Denhez, F., Detmar, M., and Goetinck, P. (2001) *J. Clin. Investig.* **107,** R9–R14
25. Elenius, V., Gotte, M., Reizes, O., Elenius, K., and Bernfield, M. (2004) *J. Biol. Chem.* **279,** 41928–41935
26. Ojeh, N., Hiilesvuo, K., Warri, A., Salmivirta, M., Henttinen, T., and Maatta, A. (2008) *J. Investig. Dermatol.* **128,** 26–34
27. Raats, C. J., Bakker, M. A., van den Born, J., and Berden, J. H. (1997) *J. Biol. Chem.* **272,** 26734–26741
28. Petersen, S. V., Oury, T. D., Ostergaard, L., Valnickova, Z., Wegrzyn, J., Thogersen, I. B., Jacobsen, C., Bowler, R. P., Fattman, C. L., Crapo, J. D., and Enghild, J. J. (2004) *J. Biol. Chem.* **279,** 13705–13710
29. Gao, F., Koenitzer, J. R., Tobolewski, J. M., Jiang, D., Liang, J., Noble, P. W., and Oury, T. D. (2008) *J. Biol. Chem.* **283,** 6058–6066
30. Oury, T. D., Crapo, J. D., Valnickova, Z., and Enghild, J. J. (1996) *Biochem. J.* **317,** 51–57
31. Fattman, C. L., Enghild, J. J., Crapo, J. D., Schaefer, L. M., Valnickova, Z., and Oury, T. D. (2000) *Biochem. Biophys. Res. Commun.* **275,** 542–548
32. Fattman, C. L., Chu, C. T., Kulich, S. M., Enghild, J. J., and Oury, T. D. (2001) *Free Radic Biol. Med.* **31,** 1198–1207
33. Pardo, A., Gibson, K., Cisneros, J., Richards, T. J., Yang, Y., Becerril, C., Yousem, S., Herrera, I., Ruiz, V., Selman, M., and Kaminski, N. (2005) *PLoS Med.* **2,** e251
34. Oury, T. D., Schaefer, L. M., Fattman, C. L., Choi, A., Weck, K. E., and Watkins, S. C. (2002) *Am. J. Physiol. Lung Cell Mol. Physiol.* **283,** L777–L784
35. Englert, J. M., Hanford, L. E., Kaminski, N., Tobolewski, J. M., Tan, R. J., Fattman, C. L., Ramsgaard, L., Richards, T. J., Loutaev, I., Nawroth, P. P., Kasper, M., Bierhaus, A., and Oury, T. D. (2008) *Am. J. Pathol.* **172,** 583–591
36. Rice, W. R., Conkright, J. J., Na, C. L., Ikegami, M., Shannon, J. M., and Weaver, T. E. (2002) *Am. J. Physiol. Lung Cell Mol. Physiol.* **283,** L256–L264
37. McQuade, K. J., Beauvais, D. M., Burbach, B. J., and Rapraeger, A. C. (2006) *J. Cell Sci.* **119,** 2445–2456
38. Zen, K., Reaves, T. A., Soto, I., and Liu, Y. (2006) *J. Immunol. Methods* **309,** 86–98
39. Enghild, J. J., Thogersen, I. B., Oury, T. D., Valnickova, Z., Hojrup, P., and Crapo, J. D. (1999) *J. Biol. Chem.* **274,** 14818–14822
40. Heit, B., Colarusso, P., and Kubes, P. (2005) *J. Cell Sci.* **118,** 5205–5220
41. Sergejeva, S., Ivanov, S., Lotvall, J., and Linden, A. (2005) *Am. J. Respir. Cell Mol. Biol.* **33,** 248–253
42. Fitzgerald, M. L., Wang, Z., Park, P. W., Murphy, G., and Bernfield, M. (2000) *J. Cell Biol.* **148,** 811–824
43. Liang, C. C., Park, A. Y., and Guan, J. L. (2007) *Nat. Protoc.* **2,** 329–333
44. Manning, C. B., Vallyathan, V., and Mossman, B. T. (2002) *Int. Immunopharmacol.* **2,** 191–200
45. Selman, M., and Pardo, A. (2002) *Respir Res.* **3,** 3
46. Kato, M., Wang, H., Kainulainen, V., Fitzgerald, M. L., Ledbetter, S., Ornitz, D. M., and Bernfield, M. (1998) *Nat. Med.* **4,** 691–697
47. Cantin, A. M., North, S. L., Fells, G. A., Hubbard, R. C., and Crystal, R. G. (1987) *J. Clin. Investig.* **79,** 1665–1673
48. Daniil, Z. D., Papageorgiou, E., Koutsokera, A., Kostikas, K., Kiropoulos, T., Papaioannou, A. I., and Gourgoulianis, K. I. (2008) *Pulm. Pharmacol. Ther.* **21,** 26–31
49. Teramoto, S., Fukuchi, Y., Uejima, Y., Shu, C. Y., and Orimo, H. (1995) *Biochem. Mol. Med.* **55,** 66–70
50. Kinder, B. W., Brown, K. K., Schwarz, M. I., Ix, J. H., Kervitsky, A., and King, T. E., Jr. (2008) *Chest* **133,** 226–232